Furrow microtubules and localized exocytosis in cleaving *Xenopus laevis* embryos

Michael V. Danilchik*, Steven D. Bedrick, Elizabeth E. Brown and Kimberly Ray

Department Biological Structure and Function SD, Oregon Health Sciences University, Portland, OR 97201-3097 USA

*Author for correspondence (e-mail: danilchi@ohsu.edu)

Accepted 10 October 2002
Journal of Cell Science 116, 273-283 © 2003 The Company of Biologists Ltd
doi:10.1242/jcs.00217

Summary

In dividing *Xenopus* eggs, furrowing is accompanied by expansion of a new domain of plasma membrane in the cleavage plane. The source of the new membrane is known to include a store of oogenetically produced exocytotic vesicles, but the site where their exocytosis occurs has not been described. Previous work revealed a V-shaped array of microtubule bundles at the base of advancing furrows. Cold shock or exposure to nocodazole halted expansion of the new membrane domain, which suggests that these microtubules are involved in the localized exocytosis. In the present report, scanning electron microscopy revealed collections of pits or craters, up to ~1.5 μm in diameter. These pits are evidently fusion pores at sites of recent exocytosis, clustered in the immediate vicinity of the deepening furrow base and therefore near the furrow microtubules. Confocal microscopy near the furrow base of live embryos labeled with the membrane dye FM1-43 captured time-lapse sequences of individual exocytotic events in which irregular patches of ~20 μm^2 of unlabeled membrane abruptly displaced pre-existing FM1-43-labeled surface. In some cases, stable fusion pores, approximately 2 μm in diameter, were seen at the surface for up to several minutes before suddenly delivering patches of unlabeled membrane. To test whether the presence of furrow microtubule bundles near the surface plays a role in directing or concentrating this localized exocytosis, membrane expansion was examined in embryos exposed to D_2O to induce formation of microtubule monasters randomly under the surface. D_2O treatment resulted in a rapid, uniform expansion of the egg surface via random, ectopic exocytosis of vesicles. This D_2O-induced membrane expansion was completely blocked with nocodazole, indicating that the ectopic exocytosis was microtubule-dependent. Results indicate that exocytotic vesicles are present throughout the egg subcortex, and that the presence of microtubules near the surface is sufficient to mobilize them for exocytosis at the end of the cell cycle.

Movies available online

Key words: Cleavage furrow, Cytokinesis, D_2O, Exocytosis, Fusion pore, Microtubule, *Xenopus*

Introduction

It is now well established that localized exocytosis occurs at or near the cytoplasmic bridge of dividing animal cells (reviewed by Straight and Field, 2000; Glotzer, 2001). That exocytosis is actually required to complete membrane separation at the end of cytokinesis is suggested in experiments with embryos of sea urchins (Conner and Wessel, 1999) and *C. elegans* (Jantsch-Plunger and Glotzer, 1999; Skop et al., 2001). In numerous organisms, this membrane insertion may have been amplified to produce the basolateral membrane domain contemporaneously with cleavage; for example, during cellularization in *Drosophila* (Sanders, 1975; Foe et al., 1993; Loncar and Singer, 1995) and during cleavage stage in a variety of large-egg organisms, including *Loligo* (Cartwright and Arnold, 1981), *Brachydanio* (Jesuthasan, 1998), sturgeon and various amphibians (Zotin, 1964; Sanders and Singal, 1975).

Amphibian embryos are distinctive among dividing cells for the comparatively large amount of membrane that is added continuously during the cleavage process (Selman and Perry, 1970). For example, in *Xenopus*, as much as 1.4 mm^2 of new plasma membrane appears in the cleavage plane during ~15 minutes of furrow progression (Bluemink and de Laat, 1973). This new membrane is known to differ qualitatively from that of the original egg surface (Kalt, 1971; Sanders and Singal, 1975; Byers and Armstrong, 1986; Servetnick et al., 1990; Bieliavsky et al., 1992; Aimar, 1997). The main source of the new membrane appears to be a pool of oogenetically produced vesicles (Leaf et al., 1990; Servetnick et al., 1990) that contributes not only membrane lipids, but also glycoproteins, and extracellular matrix components that ultimately line the surface of the blastocoel (Kalt, 1971; Servetnick et al., 1990).

How membrane expansion is regulated during cleavage is not understood. In particular, it is not yet clear where exocytosis actually takes place. It has been known since Zotin's pioneering studies in sturgeon and amphibian embryos (Zotin, 1964) that vesicles accumulate in the spindle midzone beneath the advancing first cleavage furrow, suggesting that membrane addition might occur at the leading edge of the furrow, contemporaneously with its advance through the midzone. In support of this idea, Sawai's tracing of carbon particle motions on the surface of cleaving newt eggs suggested that membrane expansion occurs from the furrow base (Sawai, 1987). Alternatively, the persistence of a stable original-membrane domain at the leading edge of the furrow, including membrane glycoproteins (Byers and Armstrong, 1986) and collections of microvilli (Denis-Donini et al., 1976), has suggested that

membrane addition occurs elsewhere along the cleavage plane, for example, at the margin between new and old domains or along its entire length. This idea has support from electron microscopic studies that show a variety of putative exocytotic vesicles at various sites along the cleavage plane, but not necessarily near its leading edge (Bieliavsky and Geuskens, 1990; Singal and Sanders, 1974).

In *Xenopus*, vesicles contributing basolaterally targeted U-cadherin to each early cleavage plane are distributed uniformly in the peripheral cytoplasm until cleavage (Angres et al., 1991). Thus, however it occurs, vesicle recruitment to the site of exocytosis must be locally regulated in the vicinity of each furrow. The possibility that microtubules might be involved in localized basolateral vesicle recruitment to the cleavage furrow was raised when Danilchik et al. (Danilchik et al., 1998) and Jesuthasan (Jesuthasan, 1998) identified novel microtubule-containing structures at the bases of cleavage furrows in *Xenopus* and *Brachydanio*, respectively. These structures are now referred to as furrow microtubule arrays (FMAs) to distinguish them from other microtubule-containing structures in the cleavage plane (e.g. midbodies and interzonal microtubules). Microtubule-disrupting experiments indicated that basolateral membrane growth in the cleavage plane requires microtubules (Danilchik et al., 1998; Jesuthasan, 1998). Similarly, Larkin and Danilchik found that furrow microtubules are required in cleaving sea urchin embryos to complete the closure of the cytoplasmic bridge, and proposed that one function of furrow microtubules is to direct vesicles toward a site of fusion at the cytoplasmic bridge to accomplish cell separation (Larkin and Danilchik, 1999). More recently, Skop et al. (Skop et al., 2001) and Shuster and Burgess (Shuster and Burgess, 2002) have identified microtubule-dependent membrane-addition events in the final stages of cytokinesis in *C. elegans* and sea urchin egg cleavage. This apparently general requirement for microtubules in the localization of membrane addition to terminate cytokinesis seems to reflect a direct recruiting of vesicles to the furrow base.

In the present report, scanning electron microscopy (SEM) and live-embryo confocal imaging revealed clusters of exocytotic fusion pores in the immediate vicinity of the expanding furrow base. Nocodazole treatment both randomized and reduced the number of these pores, indicating that microtubules are indeed required for a step in localizing vesicle exocytosis. To test whether microtubules are sufficient to direct this localization process, D_2O was used to generate ectopic microtubule monasters. D_2O-treated embryos underwent a rapid, nearly uniform expansion of the surface; SEM analysis indicated large numbers of exocytotic fusion pores randomly scattered across the entire surface. This effect of D_2O was abolished with nocodazole, confirming that microtubules near the surface, near the end of the cell cycle are sufficient to recruit exocytotic vesicles to the plasma membrane, and supporting the hypothesis that furrow microtubule bundles play a similar role in the furrows of dividing cells.

Materials and Methods

Eggs and embryos

Adult *Xenopus laevis* females were induced to ovulate with human chorionic gonadotropin (Sigma; 800 units per frog) injected into the dorsal lymph sac 18 hours prior to use (16°C). Ovulated eggs were fertilized by mixing with fragments of testis macerated in MMR/3 (MMR: 100 mM NaCl, 1.8 mM KCl, 2.0 mM $CaCl_2$, 1.0 mM $MgCl_2$, 5 mM Hepes, pH 7.5). Eggs were dejellied in 2.5% cysteine in MMR/3 at pH 8.0. Eggs were then washed free of cysteine and cultured to appropriate stages in MMR/3. For many experiments, embryos were devitellinated manually using watchmakers' forceps. This procedure was best done between 45 and 60 minutes post-fertilization to avoid mechanical rupture. Devitellinated embryos were cultured in dishes coated with 2% agarose (Type V, Sigma) to prevent membrane adherence to the substrate. In experiments involving exposure to D_2O (see below), agarose was pre-equilibrated with similar concentrations of D_2O.

Treatments

Stock solutions of nocodazole, cytochalasin B, cytochalasin D and latrunculin B (Sigma) in dimethylsulfoxide (DMSO) were diluted to concentrations of 5 or 10 μg/ml in MMR/3 and applied to embryos at specified times. Controls consisted of similar dilutions of DMSO in MMR/3. D_2O was diluted to 60% in MMR/3 and applied to embryos at specified times during early development.

Immunostaining

For examining embryos via wholemount confocal immunocytochemistry, we adapted Gard's (Gard, 1993) protocol, as described previously (Danilchik et al., 1998). Embryos were fixed for 2-4 hours at room temperature or overnight at 4°C in Gard's fixative (3.7% formaldehyde, 0.25% glutaraldehyde, 0.2% Triton X-100, 80 mM PIPES, pH 6.8, 5 mM EGTA, 1 mM $MgCl_2$). After fixation, embryos were stored in methanol overnight at –20°C. Pigmented embryos were bleached in 10% H_2O_2 in methanol on a light table for 1-4 hours (bleaching time varied, depending on rate of progress of pigment fading). After bleaching, embryos were rehydrated in three consecutive rinses, for 10 minutes each, of: 50% MeOH in TBS, 25% MeOH in TBS, 100% TBS (1× TBS: 155 mM NaCl, 20 mM Tris-Cl, pH 7.4). To decrease background fluorescence caused by glutaraldehyde and autofluorescence of yolk platelets, embryos were placed in a reducing solution of 100 mM $NaBH_4$ in TBS for 4 hours (at room temperature) or overnight (at 4°C). $NaBH_4$ was removed by rinsing in NTBS five times over the course of 1 hour (NTBS: 1× TBS, with 0.1% NP-40).

Vitelline envelopes were removed prior to exposing fixed specimens to antibody. Some embryos were bisected with a razor blade fragment, cutting parallel to the animal-vegetal axis, either perpendicular to or paralleling the cleavage plane. Other embryos were processed intact for wholemount observation. Intact or bisected embryos were incubated with antibodies diluted in TBS with 10% fetal bovine serum and 5% DMSO overnight at 4°C, with agitation, with five one-hour washes in NTBS after each incubation. Primary antibodies included monoclonals against αβ-tubulin (Biogenesis; 1:1000), γ-tubulin (Sigma; 1:200), VSVG (clone P5D4; Sigma; 1:400) and sheep polyclonal antibodies against αβ-tubulin (Cytoskeleton; 1:200). Secondary antibodies were Alexa-546- or -488-conjugated goat anti-mouse or donkey anti-sheep (Molecular Probes, 1:100). After immunostaining and subsequent washes in NTBS, embryos were dehydrated in two rinses of MeOH, 30-60 minutes each, and then cleared in two rinses of Murray's clear (2:1::benzyl benzoate:benzyl alcohol).

Surface labeling, time-lapse recording, confocal microscopy and image analysis

The growth of new membrane during cell division was visualized in devitellinated embryos exposed to fluorescent soybean agglutinin for five minutes before first cleavage (Alexa 488 conjugate; 125 μg/ml;

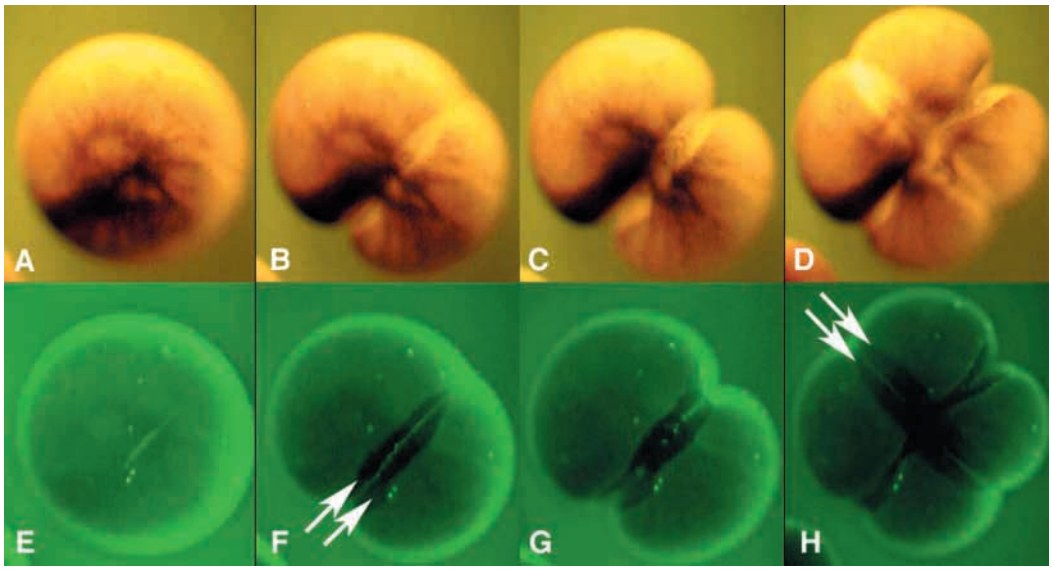

Fig. 1. Development of new basolateral domain is contemporaneous with cleavage furrowing. Embryo manually stripped of its vitelline envelope was placed on an agarose-coated surface, incubated briefly with FITC-soybean agglutinin and observed via full-spectrum (upper panels) or epifluorescence (lower panels) illumination. The new membrane domain develops as a broad, unpigmented surface along the cleavage plane (A-D). Lectin bound to the surface of devitellinated egg undergoes local concentration at onset of furrowing (bright stripe, E), followed by appearance and expansion on either side of the new, unlabelled domains of the basolateral membrane (dark areas; arrows). (H) The membrane expansion process repeats during second cleavage (arrows). Note that the new/old membrane boundary corresponds closely to the boundary between pigmented and unpigmented regions. Frames approximately 8 minutes apart.

Molecular Probes). Unbound lectin was removed via several exchanges of MMR/3 prior to time-lapse recording.

To view membrane expansion, a suspension of activated charcoal particles was pipeted over devitellinated embryos prior to time-lapse recording. Time-lapse sequences were recorded using an NEC color CCD camera mounted on an Olympus SZH stereoscope. Images were captured on a Panasonic LQ-3031 optical disk recorder, digitized via an Xclaim VR 128 graphics card (ATI), and converted to TIFF image stacks for further analysis using Wayne Rasband's NIH Image (v. 1.62; http://rsb.info.nih.gov/nih-image), or to QuickTime (Apple) movies using Quicktime Pro or Adobe Premiere 5.1.

To display carbon particle motion as a kymograph, TIFF time-lapse image stacks were opened in NIH Image, assigned a 1-pixel virtual spacing between slices, and selected regions were then rotated 90° about the Y axis to display elapsed time along the X-axis as 1 pixel per captured frame.

Exocytotic fusion pore distributions in the cleavage furrow were measured in panoramic montages of digitized SEM images across relevant surfaces registered using Adobe PhotoShop. NIH Image's particle analysis package was then used to determine pore positions relative to the base of the furrow (leading edge). Pore counts in adjacent 10 μm × 50 μm regions of interest were determined and their local density was then plotted as a function of distance from the base of the furrow.

To examine membrane dynamics in vivo at high magnification, devitellinated embryos were bathed in MMR/3 containing 10 μM cytochalasin B and 10 μM FM1-43 (Molecular Probes) and examined via confocal microscopy (BioRad Radiance 2100; Nikon E800 upright microscope using a 60×/1.0 NA CFI_{60} Fluor dipping objective). Focus on the surface of the animal hemisphere was readjusted frame by frame manually because the devitellinated embryos' height rises and falls rapidly throughout the cell cycle (Hara et al., 1980).

Scanning electron microscopy

For scanning electron microscopy, intact or devitellinated embryos were fixed in 2.5% glutaraldehyde in 0.1 M Na-cacodylate, pH 7.5 overnight at 4°C. Fixed specimens were then transferred into 0.1 M Na-cacodylate, pH 7.5 at 4°C. If necessary, embryos were manually devitellinated at this point, and then dehydrated via 15-minute exchanges with 50, 75 and 95% ethanol, followed by three 30-minute exchanges with 100% ethanol. Specimens were rinsed twice with hexamethyldisilizane (Polysciences) for 30 minutes. Specimens were then allowed to dry overnight at room temperature in open vials. More rapid, vacuum-driven removal of the hexamethyldisilizane was found to be unsatisfactory, since it often resulted in tissue contraction or surface rupture. Dried specimens were mounted onto aluminum stubs using silver paste, sputtercoated with gold-palladium to 50 nm on a Hummer VII (Analect, USA), and then examined with a JEOL T330A scanning electron microscope.

Results

In an earlier report (Danilchik et al., 1998), we suggested that furrow microtubules are involved in directing vesicles to a site of exocytosis in the growing cleavage plane. This hypothesis predicts that the site of membrane addition should be relatively near the furrow base, and that no significant membrane addition should take place elsewhere during furrow deepening. To investigate this idea, we manually removed the vitelline envelope prior to cleavage (Fig. 1A-D; Movie 1, see http://jcs.biologists.org/supplemental), making the site of membrane addition accessible for direct observation or local manipulation via microinjection of function-blocking reagents. When FITC-conjugated soybean agglutinin (FITC-SBA) was bound to the egg surface, video time-lapse recording of the redistribution of label revealed the expansion of two broad, unlabelled surface zones on both sides of the furrow midline (Fig. 1E-H). At the same time, a thin line of original-surface components became concentrated at the furrow base, a phenomenon first noted by Byers and Armstrong (Byers and Armstrong, 1986). The lectin-binding in this region probably corresponds to the tips of microvilli that remain at the furrow base (Denis-Donini et al., 1976) (see also Fig. 4B,D). The original egg surface shows remarkable coherence, with little evidence of lateral mobility of surface components, and virtually no mixing with the unlabeled domain. Evidently little

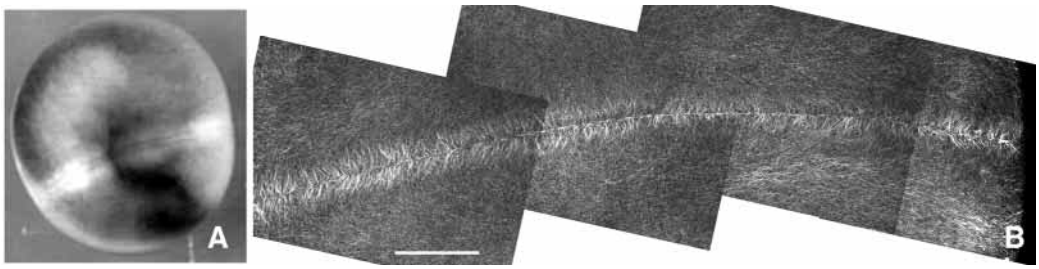

Fig. 2. Furrow microtubule bundles directly underlie the growing domain of the new membrane. (A) Furrow ceases ingression in an embryo treated with 0.1 μM latrunculin B. New membrane deposition continues, however, producing broad white stripe. (B) Same embryo, fixed and stained with antitubulin antibody. Montage is series of confocal micrographs running along cleavage furrow from animal pole to horizon. The curvature of the embryo is not apparent in montage because individual frames are single projections of image stacks, each representing several tens of microns of specimen depth. Bar, 50 μm.

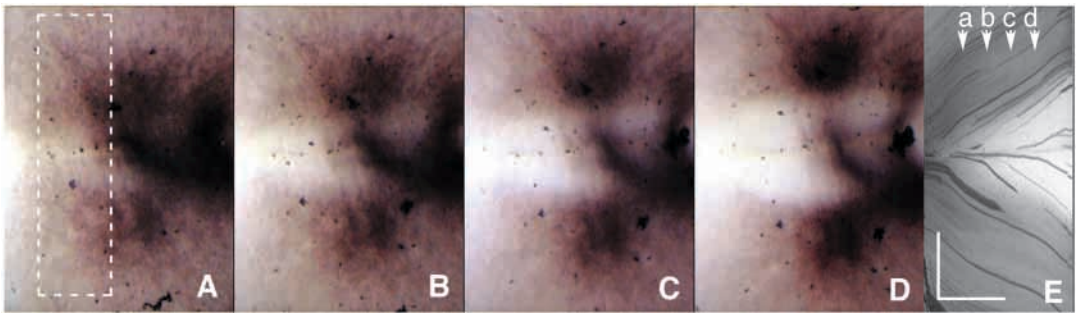

Fig. 3. Membrane expansion occurs from a site near the furrow base. A suspension of carbon particles was pipetted over the surface of devitellinated cleaving embryo. A video time-lapse sequence recorded particle movement during new membrane expansion. (A-D) Frames from the sequence, captured at 125 second intervals. (E) Kymograph made by vertically reprojecting the region of the timelapse image stack indicated by dotted box in frame A. Small arrows (a-d) indicate times in the sequence corresponding to panels A-D, respectively. Based on the parallel trajectories indicated, particles near each other travel at nearly identical speeds. Because they do not drift apart, evidently little new membrane insertion occurs between them. Vertical scale bar, 250 μm. Horizontal scale bar, 5 minutes.

or no unlabeled membrane appears in the original surface. A variety of experiments (see below) using devitellinated embryos demonstrates that the major site of membrane insertion is within 50 μm of the furrow base, and that its appearance is microtubule dependent, consistent with a role for furrow microtubules in localizing exocytosis.

Furrow microtubules underlie membrane addition site

As was earlier shown (Bluemink and de Laat, 1973; Drechsel et al., 1997; Danilchik et al., 1998), localized membrane addition continues unabated after disruption of the contractile ring by treatment with cytochalasin B or function-blocked rho protein, with the result that a broad stripe of unpigmented surface develops at the presumptive cleavage plane. Here, we show similar results with another microfilament inhibitor, latrunculin B (Fig. 2A). The same embryo fixed, processed, and stained to reveal microtubules via confocal wholemount microscopy displays prominent bundles of microtubules in close proximity to the surface (i.e. a few microns) along the entire length of the disrupted furrow (Fig. 2B). Similar results were obtained with both cytochalasin B and D.

Surface particle motions indicate site of membrane expansion

We used a method developed previously (Sawai, 1987) to follow the movement of small carbon particles dropped onto the surface of devitellinated, cleaving *Xenopus* embryos treated with cytochalasin B to expose the growing membrane domain. Video time-lapse recordings of particle motions (Fig. 3A-D) were reprocessed to produce kymographs displaying particle movement along the ordinate and elapsed time on the abscissa (Fig. 3E). Particle drift away from the furrow base was relatively steady, averaging 35 μm/minute. Particles landing near each other on the same side of the furrow traveled at nearly the same rate without drifting apart, indicating that little or no membrane expansion took place between them once they had moved beyond the furrow base. In contrast, particles landing on opposite sides of the furrow base traveled away from each other. Some particles, landing directly over the furrow base, remained there for several minutes before abruptly commencing to drift toward one side or the other. These results indicate that most of the membrane expansion occurs from a site or sites within ~50 μm of the furrow base. Similar results (not shown) were obtained in embryos not treated with cytochalasin.

Localized sites of exocytosis: scanning electron microscopy

Scanning electron microscopy was used to examine the new surface of devitellinated, cleaving embryos for evidence of exocytosis. At low magnification (Fig. 4A,C), the new membrane domains appeared as a pair of relatively smooth triangular areas on either side of the cleavage furrow (Fig. 4A). At higher magnification, surveys revealed large numbers of circular pits or craters in the otherwise smooth new-membrane domain (Fig. 4B,D). Pits ranged in size from ~0.5 to 2.0 μm in diameter. Two irregular stripes, roughly 10 μm wide, at

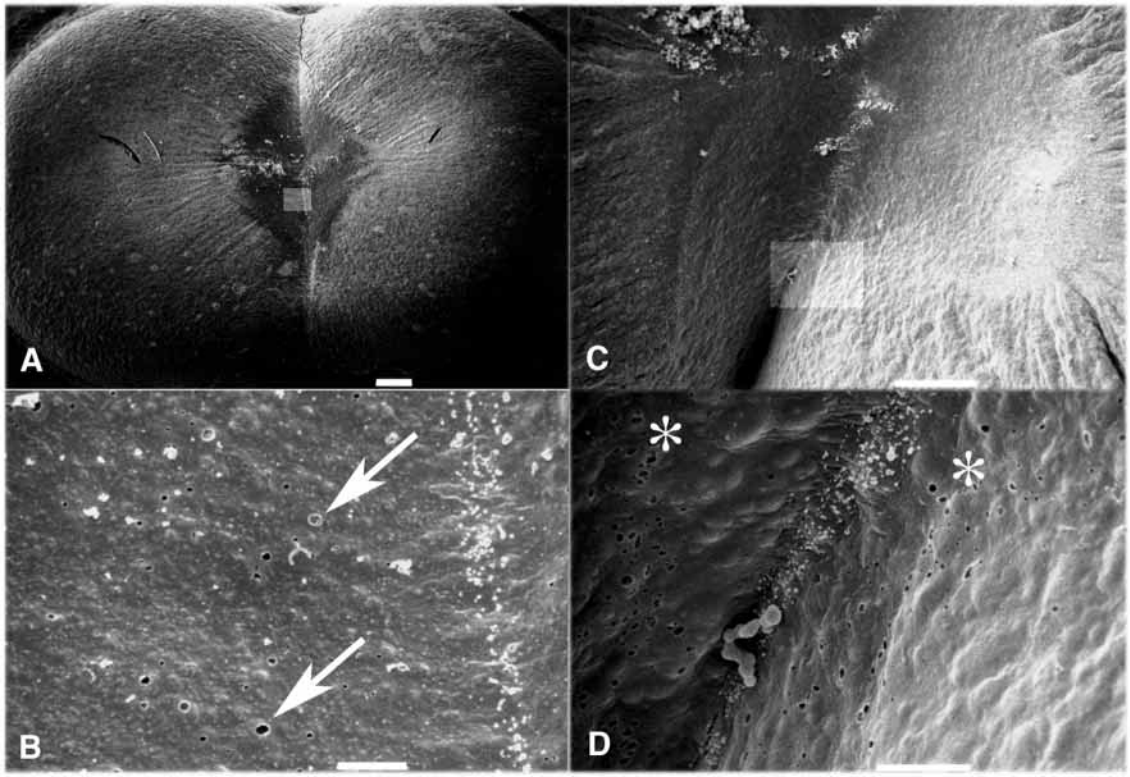

Fig. 4. SEMs of the furrow region. (A,C) Low magnification views of cleaving embryos, with a new membrane domain appearing in the furrow region. Areas indicated by boxes are shown at higher magnification in lower panels. Bars, 100 μm and 50 μm, respectively. (B,D) Region near the center of the furrow. Note the numerous pits (arrows) with raised edges appearing in clusters (asterisks) near the furrow base. Small white structures at the base of the furrow are microvilli. Bars, 10 μm.

either side of the furrow base itself were nearly devoid of pits (Fig. 4B,D). Similar analysis of embryos fixed at different times during first cleavage indicated that generally more than 75% of these pits were concentrated within 50 μm of the furrow base during the membrane expansion phase. Few pits were found near the margin between new and old membrane domains. For example, Fig. 5 (filled circles) plots pit density as a function of distance from the furrow base. In embryos treated with nocodazole during furrow formation, both the number and concentration of surface pits were significantly reduced (Fig. 5, open circles).

Localized sites of exocytosis: confocal time-lapse

The above SEM observations are consistent with the idea that the pits represent fusion pores at sites of recent or ongoing vesicle exocytosis. As an independent test of this hypothesis, we searched for evidence of exocytosis in live embryos in which the plasma membrane was loaded with the fluorescent styryl dye FM1-43. Although FM1-43 is most commonly used in pulse-chase experiments to selectively label recycling exocytotic vesicles (Betz et al., 1996), it has a relatively high affinity for new membrane in the cleavage plane of *Xenopus* embryos (see below), making it useful for identifying sites of ongoing exocytosis. Devitellinated embryos undergoing first cleavage were incubated continuously in medium containing both cytochalasin B and FM1-43. As with latrunculin (Fig. 3), the cytochalasin disrupts furrow deepening, thereby making the membrane addition site accessible for viewing by confocal microscopy (Fig. 6). FM1-43 gradually accumulated in the plasma membrane, preferentially labeling the new membrane

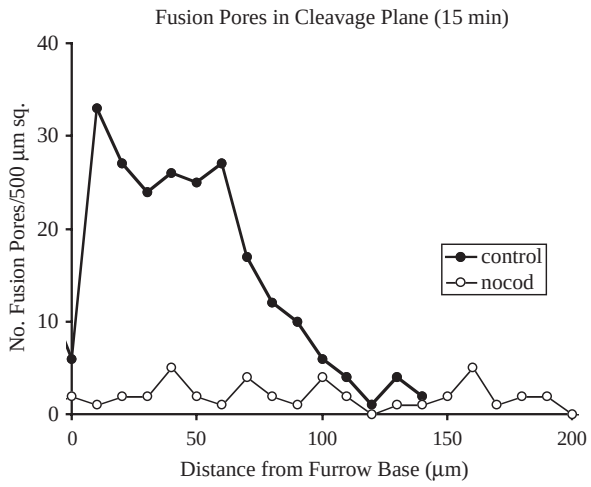

Fig. 5. Distribution of exocytotic fusion pores in the new membrane. Values refer to the number of pits counted in successive 10 μm × 50 μm regions of interest relative to the furrow base, without (closed symbols) or with (open symbols) exposure to nocodazole. The embryo was fixed 15 minutes after the beginning of the first cleavage.

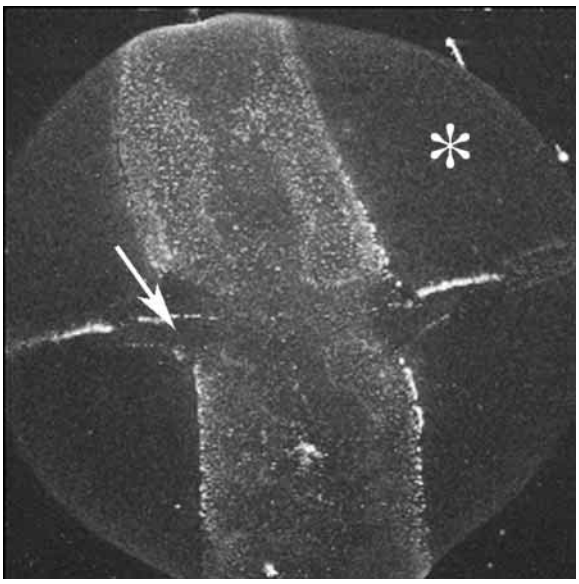

Fig. 6. Confocal image of live embryo at the beginning of the second cleavage, continuously bathed in FM1-43 and cytochalasin B. Figure shown is a flat projection of a stack of images captured through 300 μm of specimen depth. Fluorescing FM1-43 accumulates in the new membrane domain of the first cleavage plane (broad vertical stripe), but not in the original membrane domains (asterisk). Localized bright-staining puncta along the new/old membrane boundaries correspond to collections of long microvilli, and do not represent sites of endocytosis (data not shown). Membrane newly inserted along the second cleavage furrow (surrounding arrow) is momentarily less well-labeled than that previously inserted along the first furrow.

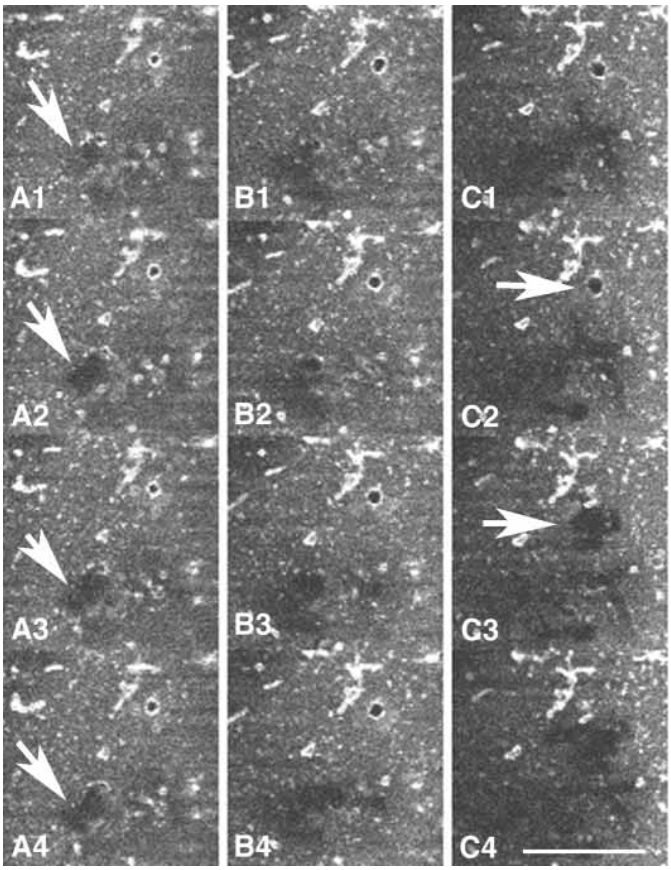

Fig. 7. Exocytosis contributes a patch of unlabeled surface to the new plasma membrane domain of an FM1-43-labeled embryo. Three representative sequences, A1-4, B1-4 and C1-4, taken from time-lapse Movie 2 (see http://jcs.biologists.org/supplemental), display a particularly active site recorded near the arrow in Fig. 6. Expanding dark regions (arrows) indicate sites of displacement of FM1-43-labeled membrane. Frames were recorded at 1.8 second intervals. Bar, 10 μm.

domain (Fig. 6, asterisk indicates less-labeled original-membrane of the animal hemisphere surface). Although some endocytosis has been detected in the new membrane domain of *Xenopus* (data not shown), consistent with recent work in zebrafish (Feng et al., 2002), the intense labeling along the margins between new and old membrane domains (Fig. 6) primarily reflects the large amount of membrane involved with microvilli and other protrusions in this region (Denis-Donini et al., 1976).

As embryos entered second cleavage, a new site of membrane addition appeared near the disrupted second furrow (arrow, Fig. 6). This expanding area was significantly less fluorescent than other regions within the new membrane domain, suggesting ongoing localized addition of unlabeled membrane. Time-lapse confocal recordings at high magnification in this region confirmed this idea. As an example, Movie 2 (see http://jcs.biologists.org/supplemental) displays a particularly active site recorded near the arrow in Fig. 6. This movie segment shows the abrupt appearance of irregular dark patches, 10-20 μm^2 in area, which quickly diffused into the surrounding FM1-43-labeled membrane. Still frames representing three successive sequences from this time-lapse recording are presented in Fig. 7. In the sequence shown in panels A1-A4, the arrows indicate a single site of membrane expansion in which a patch of unlabeled membrane abruptly grew from ~10 to 25 μm^2, before fading into the surrounding labeled surface. Similar single-fusion events are shown (Fig. 7B1-B4).

In some cases, circular structures, apparently stable exocytotic fusion pores, were seen to associate with the membrane for several minutes before abruptly flattening into the plane of the membrane and contributing unlabeled patches to it. For example, in the sequence shown in Fig. 7C1-C4, a 2.5 μm circular fluorescent structure (the same structure had also been present through the previous two sequences) suddenly disappeared to be replaced by an irregular patch of unlabeled surface (cf. arrows in Fig. 7C2-C3). The sudden introduction of the unlabeled patch evidently contributes surface area to the local membrane: by looping the movie sequence back and forth a few frames across this event, small surface particles can be seen to spread a short distance in all directions away from the patch.

A densitometric profile across the structure indicates that the membrane within the intensely labeled edges contains significantly less label than the surrounding plasma membrane (not shown). The brightly labeled edge evidently constitutes a barrier to lateral diffusion between the membrane of the vesicle and that of the cell surface until the abrupt flattening of the vesicle into the plane of the membrane.

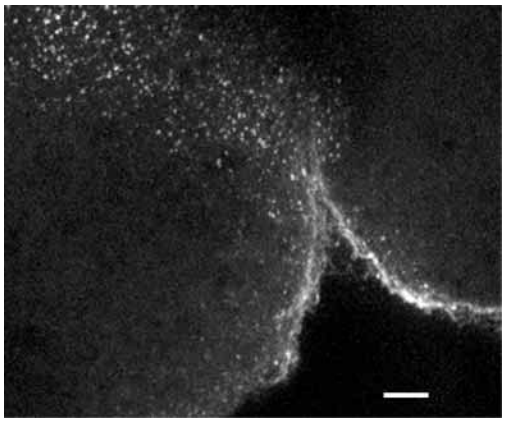

Fig. 8. VSVG-containing vesicles collect and undergo exocytosis near furrow bases. Unfertilized eggs were allowed several hours to express injected VSVG mRNA, and then were fertilized and fixed part way through the fourth cleavage. Exocytosis of labeled vesicles was exclusively along nascent basolateral surfaces lining the blastocoel. Vesicle size ranges up to 2.5 μm. Bar, 10 μm.

VSVG protein exocytosis

To learn the size range of vesicles destined for exocytosis along the basolateral surfaces, we injected fertilized eggs with capped, synthetic mRNA encoding the full-length sequence of the basolaterally targeted viral coat glycoprotein of vesicular stomatitis virus (VSVG; plasmid gift of H.-P. Moore, Berkeley, CA) and fixed and processed them for wholemount immunocytochemistry using an anti-VSVG antibody (Sigma). Fig. 8 is a projection of a confocal image stack showing a collection of VSVG-labeled vesicles near the base of a cleavage furrow. The surface is also labeled, indicating recent exocytosis of similarly labeled vesicles at or near this site. Vesicles ranged in diameter from 0.6 μm to ~2.0 μm, which is similar to the size of the presumed exocytotic pits shown above via SEM.

D_2O induces ectopic membrane expansion

We reported previously that embryos exposed to high concentrations of D_2O form numerous ectopic monasters (Danilchik et al., 1998). The concomitant disturbance in cortical pigmentation had suggested new membrane addition, consistent with the idea that the presence of polarized microtubules near the surface is sufficient to provoke new membrane addition. To examine this possibility further, we repeated our earlier experiment, this time removing the vitelline envelope prior to incubation in D_2O. The experiment shown in Fig. 9 confirms that D_2O provokes a rapid, essentially random expansion of the embryo surface. Without the support of a vitelline envelope, embryos normally flatten slightly onto the substratum and assume an oblately spheroidal morphology (Bluemink and de Laat, 1973). In contrast, in the presence of D_2O, the surface of the embryos rapidly expanded at about the time of first cleavage (Fig. 9A,B). The overall spreading and thinning of the pigmented animal hemisphere suggests that the new surface area was introduced randomly across the entire surface. Scanning EM analysis (Fig. 10) confirms that exocytotic fusion pores appeared in large numbers in the smooth surface regions between clusters of microvilli (Fig. 10B), consistent with the idea that D_2O completely randomizes the site of membrane addition. Because microvilli were retained in large numbers throughout the D_2O-driven surface expansion, it is unlikely that the observed increase in surface area is simply due to microvillar shortening.

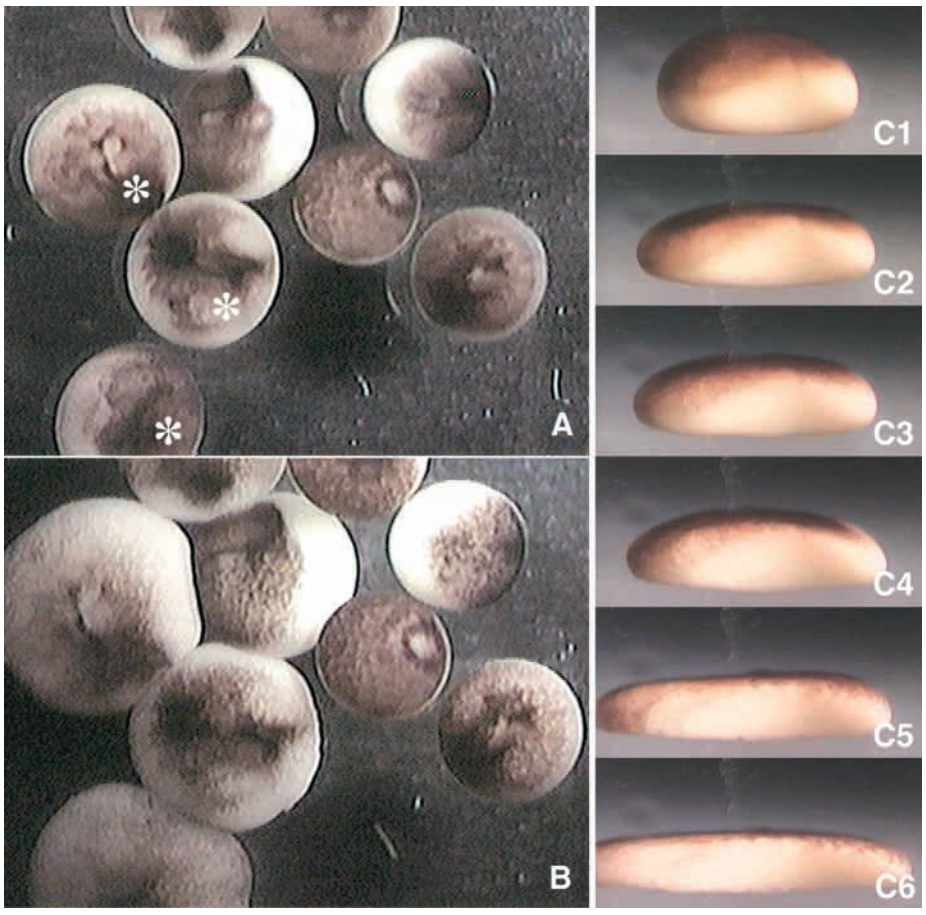

D_2O-induced expansion is blocked with nocodazole

With the appearance of new surface, the overall height of the embryo concomitantly collapsed to ~250-350

Fig. 9. D_2O-induced membrane expansion. (A) Embryos at 75 minutes post fertilization, prior to application of D_2O. Asterisks indicate embryos lacking vitelline envelopes. (B) Following 10 minutes incubation in 60% D_2O, devitellinated embryos increase their surface area and spread across the substrate. (C) Side view, obtained by recording down through a 45° prism in a culture dish. Frames are ~3 minutes apart.

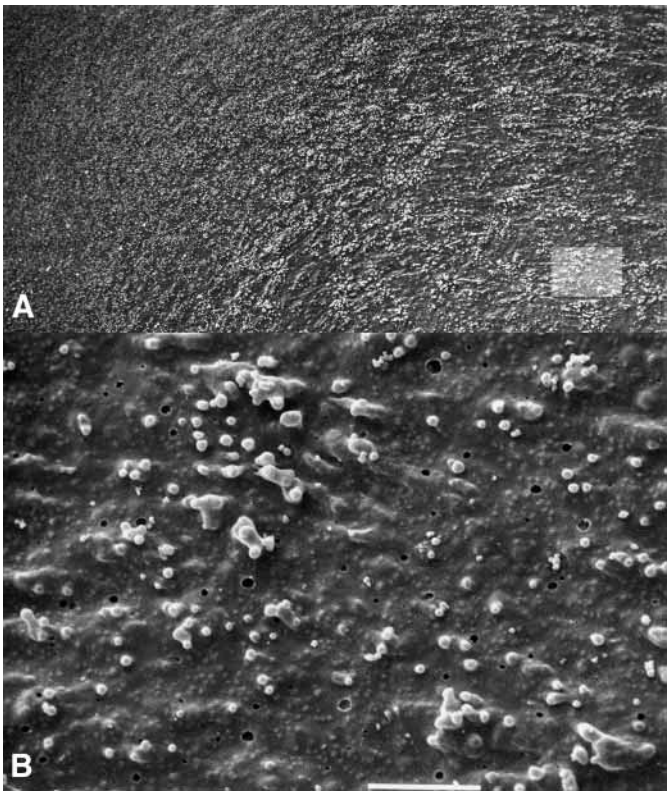

Fig. 10. Scanning EM of D_2O-treated embryo fixed during surface expansion. Low magnification (A) shows that the entire surface retains short microvilli that normally cover the embryo surface. The boxed region is shown at higher magnification in lower panel. Bar, 100 mm. Higher magnification (B) reveals random arrangement of fusion pores between collections of microvilli. Bar, 10 μm.

μm (Fig. 9C1-C6). To estimate the amount of cell surface area expansion induced by D_2O treatment, we regarded the flattening embryos as a family of progressively more oblate spheroids, with major (horizontal) and minor (vertical) axes that could be used to calculate surface areas. Radii measured across the growing horizontal profiles of the embryos yielded values for the major half-axis, 'a'. Since embryo volume (V) probably changed little during the course of an experiment, the following relationship,

$$V = \frac{4}{3}\pi a^2 b,$$

could be used to calculate the minor half-axis, 'b'. The initial embryo volume (0.85±0.03 μl) was obtained from measured horizontal diameters (1.17±0.01 mm) of nearly spherical sibling embryos still within their vitelline envelopes. Surface areas (SA) were then calculated by using

$$SA = 2\pi a^2 + \pi \frac{b^2}{\varepsilon} \ln\left(\frac{1+\varepsilon}{1-\varepsilon}\right),$$

where the eccentricity of a spheroid, ε, is described by

$$\varepsilon = \sqrt{1 - \frac{b^2}{a^2}}.$$

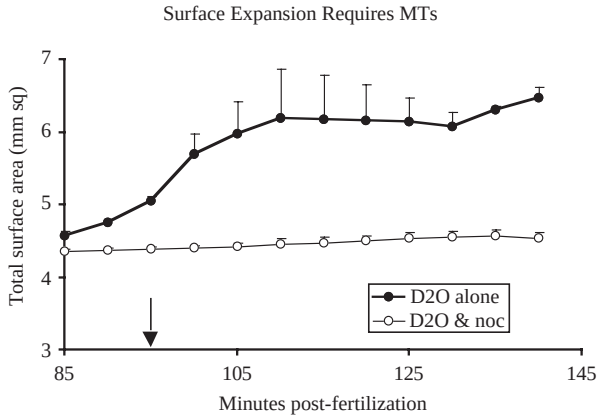

Fig. 11. D_2O-induced membrane expansion requires microtubules. Overall surface areas were calculated from measurements of horizontal profiles of embryos incubated in D_2O alone or D_2O with 10 μM nocodazole, as described in the text. Values shown are means for three embryos. The black arrow denotes onset of first cleavage in untreated sibling embryos.

Fig. 11 plots the time course of membrane expansion of D_2O-treated embryos similarly to those shown above in Fig. 9. Within approximately 15 minutes, the surface expanded by ~1.7 mm^2, an increase of nearly 40%. Most of the expansion took place at about the time that untreated controls underwent first cleavage (95 minutes post-fertilization; black arrow).

The D_2O-induced membrane expansion appears to be entirely microtubule-dependent, as indicated by the inhibition of expansion by 10 μM nocodazole (Fig. 11). To determine whether the nocodazole treatment actually disrupts microtubule formation in D_2O-treated embryos, control and treated embryos were fixed at 105 minutes post-fertilization, and examined via confocal microscopy for the presence of microtubules (Fig. 12). In an untreated embryo, aligned microtubule bundles of the FMA decorated the base of the first cleavage furrow (Fig. 12A). Elsewhere on the animal hemisphere of the same embryo, only a few microtubules were found near the surface (Fig. 12B). Vertically resectioning the same confocal stack (Fig. 12B, inset) revealed the normally low concentration of microtubules at the surface. In contrast, following treatment with D_2O, numerous microtubule monasters were found near the cell surface (Fig. 12C and vertical resection, inset). Nocodazole completely abolished microtubules in an embryo incubated in normal medium (Fig. 12D and inset), and effectively depolymerized microtubules near the surface of D_2O-treated embryos, even though monasters apparently persisted more deeply in the cytoplasm (Fig. 12E and inset). These results are consistent with a requirement for intact microtubules in membrane expansion; with the results of Figs 9-11 they indicate that the presence of microtubules near the surface is sufficient to induce membrane expansion.

Polarity of microtubules in D_2O-induced ectopic monasters

D_2O-treated embryos were double-stained for both β- and γ-tubulin and examined via confocal microscopy. Monastral microtubules were seen to extend in all directions from γ-tubulin-rich centers (Fig. 13). Since γ-tubulin is a centrosomal protein that associates with the minus ends of microtubules

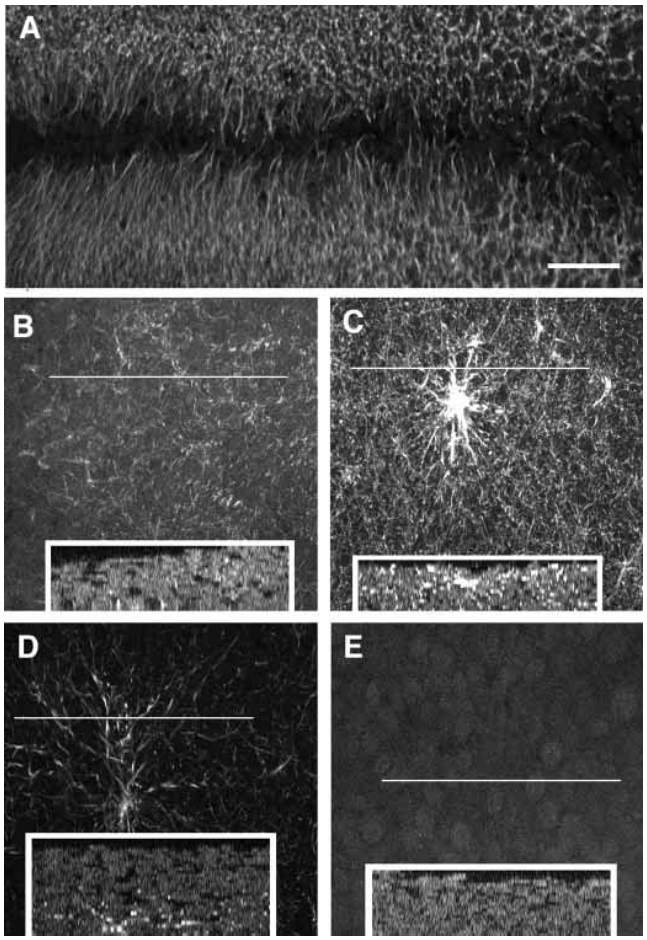

Fig. 12. Effect of D_2O and nocodazole on microtubule density near the embryo surface. Wholemount confocal microscopy of embryos stained for αβ-tubulin. (A) Furrow region of untreated cleaving embryo. (B) The same embryo, non-furrowing surface of animal hemisphere. Inset is vertical resection at the site indicated by the white horizontal line. (C) Animal surface of D_2O-treated embryo, showing through-surface view of a microtubule monaster. The inset is a vertical resection that indicates monastral microtubules are within 1 or 2 μm of the surface. (D) Nocodazole treatment completely eliminates surface microtubules. (E) Nocodazole treatment eliminates surface microtubules in a D_2O-incubated embryo. Bar, 10 μm.

(Oakley et al., 1990; Stearns et al., 1991; Stearns and Kirschner, 1994; Li and Joshi, 1995), we conclude that most of the microtubules interacting with the cortex in D_2O-treated embryos are oriented with plus ends facing the surface.

Discussion

During the first cleavage in *Xenopus*, over 1.4 mm^2 of new plasma membrane is inserted along the advancing cleavage furrow (Bluemink and de Laat, 1973). A variety of maternally synthesized membrane proteins, including U-cadherin (Angres et al., 1991), β-integrin (Gawantka et al., 1992) and other basolaterally targeted membrane proteins (Servetnick et al., 1990), appear in this new membrane domain during or shortly after membrane deposition. It is generally assumed that the surface area increase derives from the exocytosis of post-Golgi vesicles bearing these maternal proteins. However, the time course of the appearance of specific membrane proteins in the basolateral domain may not always be contemporaneous with the bulk of membrane growth itself. In *Xenopus*, Fesenko et al. (Fesenko et al., 2000) demonstrated that three maternally synthesized tight-junction proteins display three distinct different temporal expression patterns that are independent of the membrane growth itself. Also, embryonically synthesized VSVG protein appears in basolateral membranes of nocodazole-blocked *Xenopus* embryos, indicating that vesicle addition can take place passively along surfaces that are no longer growing (Roberts et al., 1992). Thus, it is clear that the exocytosis of basolateral determinants is not synonymous with the bulk expansion of membrane as the cleavage furrow advances, and it is therefore important to study membrane growth as an independent process.

The present report addressed two related issues in basolateral membrane formation during *Xenopus* cleavage: the site of membrane insertion along the furrow, and the potential role of furrow microtubules in regulating this site. We found that the bulk of membrane addition proceeds via exocytosis from a site within ~50 μm of the furrow base. This location is significant, since it overlies the ends of microtubules of the furrow microtubule array, and is therefore consistent with the idea that the microtubules mobilize the exocytotic vesicles involved in the membrane expansion. Also consistent with this hypothesis was the finding that ectopically placed microtubule plus ends near the cell surface in D_2O-treated embryos are sufficient to provoke ectopic new membrane addition. Therefore, we suggest that vesicles encountering furrow microtubules at the advancing furrow tip are transported toward the microtubule plus ends to become concentrated at either side of the base of the furrow.

Fusion pores and membrane expansion

Exocytotic fusion pores are transitory aqueous channels connecting the lumen of vesicles with the extracellular space during the process of exocytosis. As originally defined, pores

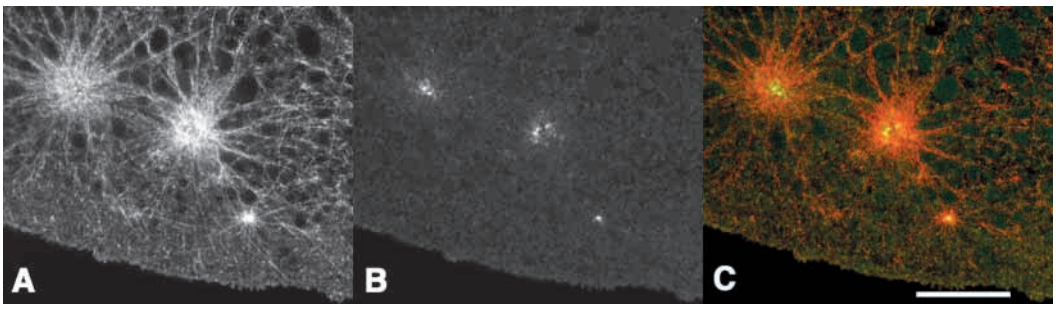

Fig. 13. Microtubules and γ-tubulin in a D_2O-treated embryo, viewed via wholemount confocal microscopy. (A) β-tubulin staining. (B) γ-tubulin staining. (C) Merged frames; red channel, β-tubulin staining; green, γ-tubulin staining. Bar, 10 μm.

are small structures, 20 to 100 nm in diameter (Breckenridge and Almers, 1987). We were initially inclined to dismiss the 2 μm pits seen via scanning EM as fixation artefacts. However, their nonrandom distribution, relatively uniform size range, and absence under conditions preventing new membrane addition (e.g. nocodazole) suggested that they might represent authentic exocytotic fusion pores. Similar structures in the 2 μm diameter range, observed via SEM in secretory alveolar type II cells, are accepted as authentic fusion pores, with channels remaining open for up to several hours (Haller et al., 2001). Similarly, large, stable cortical crypts or pits remain in the surface for several minutes following cortical granule exocytosis in zebrafish (Becker and Hart, 1999).

By independent methods, we visualized 2 μm hollow cavities in the growing surface of living embryos that resemble those seen in SEM. Time-lapse confocal microscopy of embryos stained with FM1-43 gave us a glimpse of the dynamic, transitory nature of these exocytotic fusion pores. Some apparently stable fusion pores remained at the surface for up to several minutes before flattening into the plane of the cell surface as a patch of unlabeled membrane. The area of each patch was approximately 10-20 μm^2, an amount of surface that could have been provided by individual vesicles ranging in diameter from ~2.2 to 2.8 μm. We asked whether the density of fusion pores seen in cleavage furrows could provide a sufficient number of exocytotic events to account for the large amount of membrane introduced during cleavage. Bluemink and de Laat (Bluemink and de Laat, 1973) estimated that ~2.3 mm^2 of new membrane is introduced ectopically to the surface following cytochalasin B treatment. Our embryos were smaller than those used by Bluemink and de Laat (1.16 mm diameter); we estimate the total new membrane in our cytochalasin-treated embryos (Fig. 6) to be ~1.85 mm^2. Assuming that each fusion pore represents a potential delivery of 20 μm^2, as suggested from the FM1-43 labeling experiment (Fig. 7C), then ~92,500 vesicles would be needed. Since membrane addition is continuous over a period lasting ~15 minutes, only a limited number of fusion pores should be seen at any time in fixed SEM specimens. The profile of fusion pore density in Fig. 5 shows 27±3 fusion pores per adjacent 500 μm^2 regions nearest the furrow base. Again, if each pore represents 20 μm^2 of potential surface area, this density of exocytotic vesicles could represent ~99,000 vesicles. In other words, the fusion pore clusters near the furrow base are of a density consistent with that capable of providing the entire 1.85 mm^2.

Microtubule polarity

D_2O-stabilized microtubules appear to be fully capable of supporting organelle transport in *Xenopus* embryos, in a reportedly 'randomized' fashion (Rowning et al., 1997). However, as we have shown here, D_2O-stabilized microtubules are evidently not randomized; instead, they form well-organized, ectopic monasters (see also Danilchik et al., 1998). The presence of centriole-like structures (van Assel and Brachet, 1966) and, as shown in this report, γ-tubulin at the foci of these monasters, indicate that the D_2O-stabilized monasters resemble conventional MTOCs, with microtubule plus ends radiating away from organizing centers. In effect, the entire cortex becomes enriched with overlapping arrays of microtubule plus ends, a situation that normally only occurs along the cleavage plane. Since the effect of D_2O on membrane expansion is blocked with nocodazole, we conclude that the exocytosis of vesicles depends on a plus-ward transport of vesicles. This conclusion is thus consistent with that of experiments demonstrating kinesin-dependence in the microtubule-based mobilization of vesicles toward sites of wound-induced exocytosis (Bi et al., 1997).

We still lack direct information about the polarity of microtubules in the FMA. From the SEM data shown here, we know that the site of membrane addition is just to either side of the furrow base, making it unlikely that the FMA transports vesicles toward the midline. Rather, the observed sites of exocytosis are consistent with vesicles being transported away from the midline. However, this leads to a surprising result: if exocytotic vesicles are indeed plus-directed, as suggested by the D_2O experiments, then the FMA bundles should be oriented with minus ends toward the midline. Such a microtubular arrangement is clearly in conflict with the known organization of plant-cell phragmoplasts (Staehelin and Hepler, 1996) and animal-cell midbodies (Eutenauer and McIntosh, 1980). To resolve this issue, we are presently investigating the polarity of FMA microtubules by following the motion of GFP-tagged EB1 in cleaving *Xenopus* embryos (E.E.B. and M.V.D., unpublished).

We thank Jerry Adey and Kay Larkin for help with the scanning electron microscopy. This work was supported by the National Science Foundation (IBN-0110985 and DBI-0070391) and by the National Aeronautics and Space Administration (NAG2-1199).

References

Aimar, C. (1997). Formation of new plasma membrane during the first cleavage cycle in the egg of *Xenopus laevis*: an immunocytological study. *Dev. Growth Differ.* **39**, 693-704.

Angres, B., Muller, A. H., Kellermann, J. and Hausen, P. (1991). Differential expression of two cadherins in *Xenopus laevis*. *Development* **111**, 829-844.

Becker, K. A. and Hart, N. H. (1999). Reorganization of filamentous actin and myosin-II in zebrafish eggs correlates temporally and spatially with cortical granule exocytosis. *J. Cell Sci.* **112**, 97-110.

Betz, W. J., Mao, F. and Smith, C. B. (1996). Imaging exocytosis and endocytosis. *Curr. Opin. Neurobiol.* **6**, 365-371.

Bi, G.-Q., Morris, R. L., Liao, G., Alderton, J. M., Scholey, J. M. and Steinhardt, R. A. (1997). Kinesin- and myosin-driven steps of vesicle recruitment for Ca2+ regulated exocytosis. *J. Cell Biol.* **138**, 999-1008.

Bieliavsky, N. and Geuskens, M. (1990). Interblastomeric plasma membrane formation during cleavage of *Xenopus laevis* embryos. *J. Submicrosc. Cytol. Pathol.* **22**, 445-457.

Bieliavsky, N., Geuskens, M., Goldfinger, M. and Tencer, R. (1992). Isolation of plasma membranes, Golgi bodies and mitochondria of *Xenopus laevis* morulae. Identification of plasma membrane proteins. *J. Submicrosc. Cytol. Pathol.* **24**, 335-349.

Bluemink, J. G. and de Laat, S. W. (1973). New membrane formation during cytokinesis in normal and cytochalasin B-treated eggs of *Xenopus laevis*. I. Electron microscope observations. *J. Cell Biol.* **59**, 89-108.

Breckenridge, L. J. and Almers, W. (1987). Final steps in exocytosis observed in a cell with giant secretory granules. *Proc. Natl. Acad. Sci. USA* **84**, 1945-1949.

Byers, T. J. and Armstrong, P. B. (1986). Membrane protein redistribution during *Xenopus* first cleavage. *J. Cell Biol.* **102**, 2176-2184.

Cartwright, J., Jr and Arnold, J. M. (1981). Intercellular bridges in the embryo of the Atlantic squid, *Loligo pealei*. II: Formation of the bridge. *Cell Motility* **1**, 455-468.

Conner, S. D. and Wessel, G. M. (1999). Syntaxin is required for cell division. *Mol Biol Cell* **10**, 2735-2743.

Danilchik, M. V., Funk, W. C., Brown, E. E. and Larkin, K. (1998). Requirement for microtubules in new membrane formation during cytokinesis of Xenopus embryos. *Dev. Biol.* **194**, 47-60.

Denis-Donini, S., Baccetti, B. and Monroy, A. (1976). Morphological changes of the surface of the eggs of *Xenopus laevis* in the course of development. 2. Cytokinesis and early cleavage. *J. Ultrastruct. Res.* **57**, 104-112.

Drechsel, D. N., Hyman, A. A., Hall, A. and Glotzer, M. (1997). A requirement for Rho and Cdc42 during cytokinesis in Xenopus embryos. *Curr. Biol.* **7**, 12-23.

Euteneuer, U. and McIntosh, J. R. (1980). Polarity of midbody and phragmoplast microtubules. *J. Cell Biol.* **87**, 509-515.

Feng, B., Schwarz, H. and Jesuthasan, S. (2002). Furrow-specific endocytosis during cytokinesis of zebrafish blastomeres. *Exp. Cell Res.* **279**, 14-20.

Fesenko, I., Kurth, T., Sheth, B., Fleming, T. P., Citi, S. and Hausen, P. (2000). Tight junction biogenesis in the early *Xenopus* embryo. *Mech. Dev.* **96**, 51-65.

Foe, V. E., Odell, G. M. and Edgar, B. A. (1993). Mitosis and morphogenesis in the Drosophila embryo. In *The Development of Drosophila melanogaster*, pp. 149-300. Woodbury, NY: Cold Spring Harbor Laboratory Press.

Gard, D. L. (1993). Confocal immunofluorescence microscopy of microtubules in amphibian oocytes and eggs. *Methods Cell Biol.* **38**, 241-264.

Gawantka, V., Ellinger-Ziegelbauer, H. and Hausen, P. (1992). Beta 1-integrin is a maternal protein that is inserted into all newly formed plasma membranes during early Xenopus embryogenesis. *Development* **115**, 595-605.

Glotzer, M. (2001). Animal cell cytokinesis. *Annu. Rev. Cell Dev. Biol.* **17**, 351-386.

Haller, T., Dietl, P., Pfaller, K., Frick, M., Mair, N., Paulmichl, M., Hess, M. W., Furst, J. and Maly, K. (2001). Fusion pore expansion is a slow, discontinuous, and Ca2+-dependent process regulating secretion from alveolar type II cells. *J. Cell Biol.* **155**, 279-289.

Hara, K., Tydeman, P. and Kirschner, M. (1980). A cytoplasmic clock with the same period as the division cycle in Xenopus eggs. *Proc. Natl. Acad. Sci. USA* **77**, 462-466.

Jantsch-Plunger, V. and Glotzer, M. (1999). Depletion of syntaxins in the early Caenorhabditis elegans embryo reveals a role for membrane fusion events in cytokinesis. *Curr. Biol.* **9**, 738-745.

Jesuthasan, S. (1998). Furrow-associated microtubule arrays are required for the cohesion of zebrafish blastomeres following cytokinesis. *J. Cell Sci.* **111**, 3695-3703.

Kalt, M. R. (1971). The relationship between cleavage and blastocoel formation in *Xenopus laevis*. II. Electron microscopic observations. *J. Embryol. Exp. Morphol.* **26**, 51-66.

Larkin, K. and Danilchik, M. V. (1999). Microtubules are required for completion of cytokinesis in sea urchin eggs. *Dev. Biol.* **214**, 215-226.

Leaf, D. S., Roberts, S. J., Gerhart, J. C. and Moore, H. P. (1990). The secretory pathway is blocked between the trans-Golgi and the plasma membrane during meiotic maturation in Xenopus oocytes. *Dev. Biol.* **141**, 1-12.

Li, Q. and Joshi, H. C. (1995). gamma-tubulin is a minus end-specific microtubule binding protein. *J. Cell Biol.* **131**, 207-214.

Loncar, D. and Singer, S. J. (1995). Cell membrane formation during the cellularization of the syncytial blastoderm of Drosophila. *Proc. Natl. Acad. Sci. USA* **92**, 2199-2203.

Oakley, B. R., Oakley, C. E., Yoon, Y. and Jung, M. K. (1990). Gamma tubulin is a component of the spindle pole body that is essential for microtubule function in *Aspergillus nidulans*. *Cell* **61**, 1289-1301.

Roberts, S. J., Leaf, D. S., Moore, H. P. and Gerhart, J. C. (1992). The establishment of polarized membrane traffic in *Xenopus laevis* embryos. *J. Cell Biol.* **118**, 1359-1369.

Rowning, B. A., Wells, J., Wu, M., Gerhart, J. C., Moon, R. T. and Larabell, C. A. (1997). Microtubule-mediated transport of organelles and localization of beta- catenin to the future dorsal side of Xenopus eggs. *Proc. Natl. Acad. Sci. USA* **94**, 1224-1229.

Sanders, E. J. (1975). Aspects of furrow membrane formation in the cleaving Drosophila embryo. *Cell Tissue Res.* **156**, 463-474.

Sanders, E. J. and Singal, P. K. (1975). Furrow formation in Xenopus embryos. Involvement of the golgi body as revealed by ultrastructural localization of thiamine pyrophosphatase activity. *Exp. Cell Res.* **93**, 219-224.

Sawai, T. (1987). Surface movement in the region of the cleavage furrow of amphibian eggs. *Zool. Sci.* **4**, 825-832.

Selman, G. G. and Perry, M. M. (1970). Ultrastructural changes in the surface layers of the newt's egg in relation to the mechanism of its cleavage. *J. Cell Sci.* **6**, 207-227.

Servetnick, M., Schulte-Merker, S. and Hausen, P. (1990). Cell surface proteins during early *Xenopus* development: Analysis of cell surface proteins and total glycoproteins provides evidence of a maternal glycoprotein pool. *Roux. Arch. Dev. Biol.* **198**, 433-442.

Shuster, C. B. and Burgess, D. R. (2002). Targeted new membrane addition in the cleavage furrow is a late, separate event in cytokinesis. *Proc. Natl. Acad. Sci. USA* **99**, 3633-3638.

Singal, P. K. and Sanders, E. J. (1974). An ultrastructural study of the first cleavage of Xenopus embryos. *J. Ultrastruct. Res.* **47**, 433-451.

Skop, A. R., Bergmann, D., Mohler, W. A. and White, J. G. (2001). Completion of cytokinesis in C. elegans requires a brefeldin A- sensitive membrane accumulation at the cleavage furrow apex. *Curr. Biol.* **11**, 735-746.

Staehelin, L. A. and Hepler, P. K. (1996). Cytokinesis in higher plants. *Cell* **84**, 821-824.

Stearns, T. and Kirschner, M. (1994). In vitro reconstitution of centrosome assembly and function: the central role of gamma-tubulin. *Cell* **76**, 623-637.

Stearns, T., Evans, L. and Kirschner, M. (1991). Gamma-tubulin is a highly conserved component of the centrosome. *Cell* **65**, 825-836.

Straight, A. F. and Field, C. M. (2000). Microtubules, membranes and cytokinesis. *Curr Biol* **10**, R760-R770.

van Assel, S. and Brachet, J. (1966). The formation of cytasters in amphibian eggs after treatment with heavy water. *J. Embryol. Exp. Morphol.* **15**, 143-151.

Zotin, A. I. (1964). The mechanism of cleavage in amphibian and sturgeon eggs. *J. Embryol. Exp. Morphol.* **12**, 247-262.